

Photon+jets measurements at D0

Dmitry V. Bandurin

Kansas State University, Kansas, Manhattan, KS 66506, USA

In this paper, we present a few measurements done at the D0 experiment at the Fermilab Tevatron Collider. These measurements include the triple differential cross sections ($d^3\sigma/dp_T^\gamma dy^\gamma dy^{\text{jet}}$) of the photon and associated jet production, the photon and heavy flavour (b and c) jet, and finally, study of the event with double parton scattering using $\gamma+3$ jet events. Each section below presents a brief description of those measurements and results.

I. MEASUREMENT OF THE DIFFERENTIAL CROSS SECTION FOR THE PRODUCTION OF AN ISOLATED PHOTON WITH ASSOCIATED JET IN $p\bar{p}$ COLLISIONS AT $\sqrt{s}=1.96$ TEV

The production of a photon with associated jets in the final state is a powerful probe of the dynamics of hard QCD interactions [1]. Different angular configurations between the photon and the jets can be used to extend inclusive photon production measurements and simultaneously test the underlying dynamics of QCD hard-scattering subprocesses in different regions of parton momentum fraction x and large hard-scattering scales Q^2 .

Here we present an analysis of photon plus jets production in $p\bar{p}$ collisions at a center-of-mass energy $\sqrt{s}=1.96$ TeV in which the most-energetic (leading in p_T) photon is produced centrally with a rapidity $|y^\gamma| < 1.0$ [2]. The cross section as a function of photon transverse momentum p_T^γ is measured differentially for four separate angular configurations of the highest p_T (leading) jet and the leading photon rapidities. The leading jet is required to be in either the central ($|y^{\text{jet}}| < 0.8$) or forward ($1.5 < |y^{\text{jet}}| < 2.5$) rapidity intervals, with $p_T^{\text{jet}} > 15$ GeV. The four angular configurations studied are: central jets with $y^\gamma \cdot y^{\text{jet}} > 0$ and with $y^\gamma \cdot y^{\text{jet}} < 0$, and forward jets with $y^\gamma \cdot y^{\text{jet}} > 0$ and with $y^\gamma \cdot y^{\text{jet}} < 0$. The total x and Q^2 region covered by the measurement is $0.007 \lesssim x \lesssim 0.8$ and $900 \leq Q^2 \equiv (p_T^\gamma)^2 \leq 1.6 \times 10^5$ GeV², extending the kinematic reach of previous photon plus jet measurements (see refs. inside [2]). Ratios between the differential cross sections in the four studied angular configurations are also presented. The measurements are compared to the corresponding theoretical predictions.

The data presented here correspond to an integrated luminosity of 1.01 ± 0.06 fb⁻¹ collected using the D0 detector [3] at the Fermilab Tevatron $p\bar{p}$ collider operating at a center-of-mass energy $\sqrt{s}=1.96$ TeV.

Events containing at least one hadronic jet are selected. Jets are reconstructed using the D0 Run II jet-finding algorithm with a cone of radius 0.7 [4], and are required to satisfy quality criteria which suppress background from leptons, photons, and detector noise

effects. Jet energies are corrected to the particle level.

In total, about 1.4 million candidate events are selected after application of all selection criteria. A correction for the “ γ +jet” event purity \mathcal{P} is then applied to account for the remaining background in the region $O_{\text{NN}} > 0.7$. The distribution of the ANN output for the simulated photon signal and dijet background samples are fitted to the data for each p_T^γ bin using a maximum likelihood fit [5] to obtain the fractions of signal and background components. The found purities vary as 0.52 – 0.99 for $30 < p_T^\gamma < 400$ GeV.

The data are compared to next-to-leading order (NLO) QCD predictions obtained using JETPHOX [7], with CTEQ6.5M PDF [6] and BFG fragmentation functions of partons to photons [8]. The renormalization, factorization, and fragmentation scales (μ_R , μ_F , and μ_f) are set equal to $p_T^\gamma f(y^*)$, where $f(y^*) = \{[1 + \exp(-2|y^*|)]/2\}^{1/2}$ and $y^* = 0.5(y^\gamma - y^{\text{jet}})$ [9].

The prediction using the CTEQ6.5M PDF and BGF fragmentation sets does not describe the shape of the cross section over the whole measured range. In particular, the prediction is above the data for events with $|y^{\text{jet}}| < 0.8$ in the region $p_T^\gamma > 100$ GeV and below the data for jets produced in the $1.5 < |y^{\text{jet}}| < 2.5$, $y^\gamma \cdot y^{\text{jet}} > 0$ rapidity region for $p_T^\gamma < 50$ GeV. Most of the data points in these p_T^γ and rapidity regions are (1–1.5) $\delta\sigma_{\text{tot}}$ outside of the CTEQ6.5M PDF set uncertainty range which is shown by the shaded region in the figure and calculated according to the prescription in [6]. Note that the data-to-theory ratios have a shape similar to those observed in the inclusive photon cross sections measured by the UA2 [10], CDF [11] and D0 [12] collaborations.

The experimental systematic uncertainties are reduced further by measuring the ratios between the differential cross sections $D = d^3\sigma/dp_T^\gamma dy^\gamma dy^{\text{jet}}$ in the different regions. Most of the systematic uncertainties related to the identification of central photons then cancel, and only systematic uncertainties related to the $p\bar{p} \rightarrow \gamma + \text{jet} + X$ event purities and the jet selection efficiency (when measuring ratios between central and forward jet regions) remain. Measured ratios between the differential cross sections in the different regions are presented in Fig. 2. The ratios also significantly reduces theoretical scale uncertainties [2]. The shapes of the measured ratios between the cross sections in the different regions, in general, are qualita-

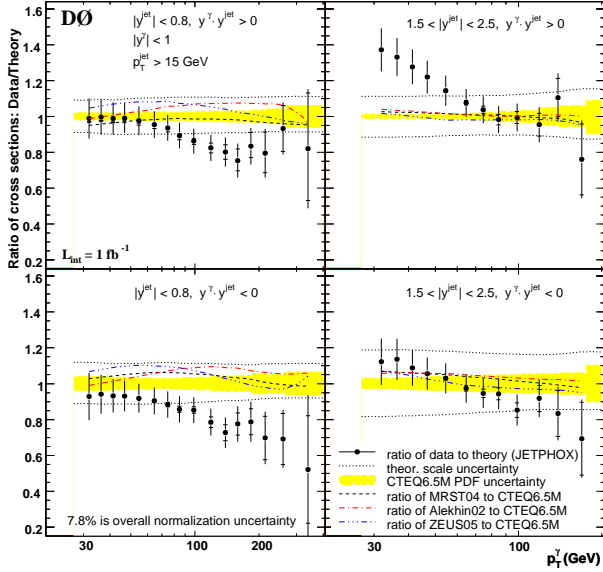


FIG. 1: The ratios of the measured triple-differential cross section, in each measured interval, to the NLO QCD prediction using JETPHOX [7] with the CTEQ6.5M PDF set and all three scales $\mu_{R,F,f} = p_T^\gamma f(y^*)$. The solid vertical line on the points shows the statistical and p_T -dependent systematic uncertainties added in quadrature, while the internal line shows the statistical uncertainty. The two dotted lines represent the effect of varying the theoretical scales by a factor of two.

tively reproduced by the theory. A quantitative difference, however, between theory and the measurement is observed for the ratios of the central jet regions to the forward $1.5 < |y^{\text{jet}}| < 2.5$, $y^\gamma \cdot y^{\text{jet}} > 0$ region, even after the theoretical scale variation is taken into account. The ratio between the two forward jet cross sections suggests a scale choice $\mu_{R,F,f} \simeq 2p_T^\gamma f(y^*)$. However, the ratios of the central jet regions to the forward $1.5 < |y^{\text{jet}}| < 2.5$, $y^\gamma \cdot y^{\text{jet}} < 0$ region suggest a theoretical scale closer to $\mu_{R,F,f} \simeq 0.5p_T^\gamma f(y^*)$.

II. MEASUREMENT OF $\gamma + b + X$ AND $\gamma + c + X$ PRODUCTION CROSS SECTIONS IN $p\bar{p}$ COLLISIONS AT $\sqrt{s} = 1.96$ TEV

Photons produced in association with heavy quarks Q ($\equiv c$ or b) in the final state of hadron-hadron interactions provide valuable information about the parton distributions of the initial state hadrons [13, 14]. Such events are produced primarily through the QCD Compton-like scattering process $gQ \rightarrow \gamma Q$ but also through quark-antiquark annihilation $q\bar{q} \rightarrow \gamma g \rightarrow \gamma Q\bar{Q}$. Consequently, $\gamma + Q + X$ production is sensitive to the b , c , and gluon (g) densities within the colliding hadrons, and can provide constraints on parton distribution functions that have substantial uncertainties [6]. The heavy quark and gluon content is an

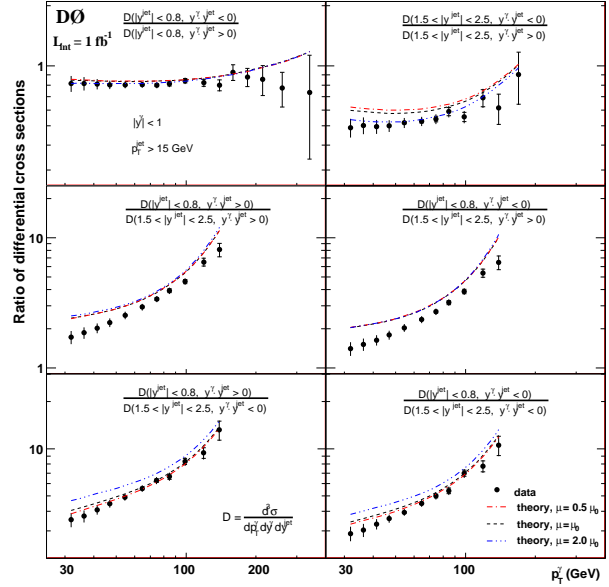


FIG. 2: The ratios between the differential cross sections in each y^{jet} region. The solid vertical error bars correspond to the statistical and systematic uncertainties added in quadrature while the horizontal marks indicate the statistical uncertainty. NLO QCD theoretical predictions for the ratios, estimated using JETPHOX, are shown for three different scales: $\mu_{R,F,f} = \mu_0, 0.5\mu_0$, and $2\mu_0$, where $\mu_0 = p_T^\gamma f(y^*)$.

important aspect of QCD dynamics and of the fundamental structure of the proton. In particular, many searches for new physics, e.g. for certain Higgs boson production modes [15, 16, 17], will benefit from the increased PDF precision with respect to the heavy quark and gluon content of the proton.

This section presents the first measurements of the inclusive differential cross sections $d^3\sigma / (dp_T^\gamma dy^\gamma dy^{\text{jet}})$ for $\gamma + b + X$ and $\gamma + c + X$ production in $p\bar{p}$ collisions, where y^γ and y^{jet} are the photon and jet rapidities [18]. The results are based on an integrated luminosity of $1.02 \pm 0.06 \text{ fb}^{-1}$ collected with the D0 detector at the Fermilab Tevatron Collider at $\sqrt{s} = 1.96$ TeV. The highest p_T (leading) photon and jet are required to have $|y^\gamma| < 1.0$ and $|y^{\text{jet}}| < 0.8$, and transverse momentum $30 < p_T^\gamma < 150$ GeV and $p_T^{\text{jet}} > 15$ GeV. This selection allows one to probe PDFs in the range of parton-momentum fractions (x) $0.01 \lesssim x \lesssim 0.3$, and hard scatter scales of $9 \times 10^2 \lesssim Q^2 \equiv (p_T^\gamma)^2 \lesssim 2 \times 10^4 \text{ GeV}^2$. Differential cross sections are presented for two regions of kinematics, defined by $y^\gamma \cdot y^{\text{jet}} > 0$ and $y^\gamma \cdot y^{\text{jet}} < 0$. These two regions provide greater sensitivity to the parton x because they probe different sets of x_1 and x_2 intervals, as discussed in [2].

Photon selection criteria and methods for estimating photon purities are similar to those used in [2]. At least one jet must be present in each event. Jets

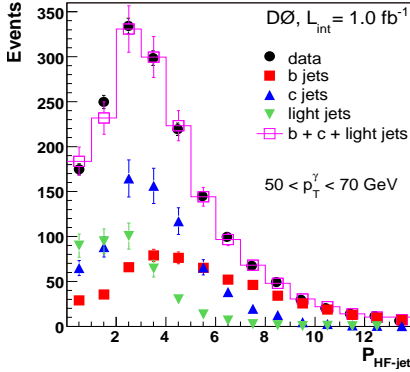


FIG. 3: Distribution of observed events for $P_{\text{HF-jet}}$ after all selection criteria for the bin $50 < p_T^\gamma < 70$ GeV. The distributions for the b , c , and light jet templates are shown normalized to their fitted fraction. Error bars on the templates represent combined uncertainties from statistics of the MC and the fitted jet flavor fractions, while the data contain just statistical uncertainties. Fits in the other p_T^γ bins are of similar quality.

are reconstructed using the D0 Run II algorithm [4] with a radius of 0.5. Light jets are suppressed using a dedicated artificial neural network (b -ANN) [19] that exploits the longer lifetimes of heavy-flavor hadrons relative to their lighter counterparts. The leading jet is required to have a b -ANN output value > 0.85 .

About 13,000 events remain in the data sample after applying all selection criteria. To estimate the photon purity, the γ -ANN distribution in data is fitted to a linear combination of templates for photons and jets obtained from simulated $\gamma + \text{jet}$ and dijet samples, respectively. An independent fit is performed in each p_T^γ bin, yielding photon purities between 51% and 93% for $30 < p_T^\gamma < 150$ GeV. The fractional contributions of b and c jets are determined by fitting templates of $P_{\text{HF-jet}} = -\ln \prod_i P_{\text{track}}^i$ to the data, where P_{track}^i is the probability that a track originates from the primary vertex, based on the significance of the track's distance of closest approach to the primary vertex. Templates are used for the shape information of the $P_{\text{HF-jet}}$ distributions. For b and c jets these are extracted from MC events while the light jet template is taken from a data sample enriched in light jets, which is corrected for contributions from b and c quarks.

The result of a maximum likelihood fit, normalized to the number of events in data, is shown in Fig. 3 for $50 < p_T^\gamma < 70$ GeV, as an example. The estimated fractions of b and c jets in all p_T^γ bins vary between 25–34% and 40–48%, respectively. The corresponding uncertainties range between 7–24%, dominated at higher p_T^γ by the limited data statistics.

The measured differential cross sections are shown in Fig. 4 for $\gamma + b + X$ and $\gamma + c + X$ production as a function of p_T^γ for the jet and photon rapidity intervals in question. The cross sections fall by more than three

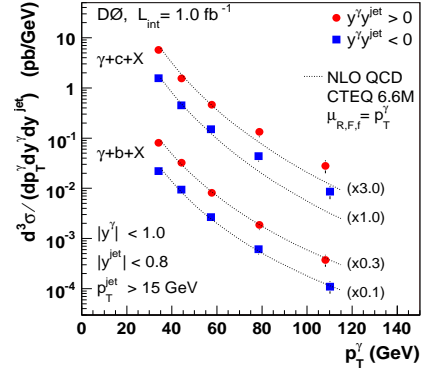


FIG. 4: The $\gamma + b + X$ and $\gamma + c + X$ differential cross sections as a function of p_T^γ in the two regions $y^\gamma y^{\text{jet}} > 0$ and $y^\gamma y^{\text{jet}} < 0$. The uncertainties on the data points include statistical and systematic contributions added in quadrature. The NLO pQCD predictions using CTEQ6.6M PDFs are indicated by the dotted lines.

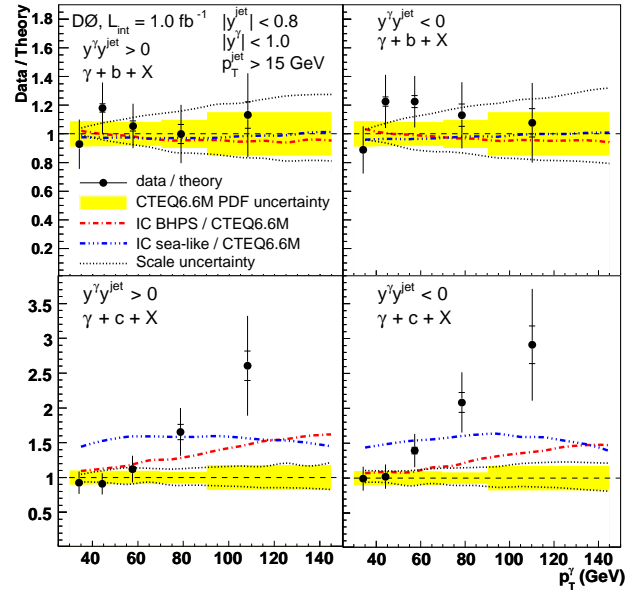


FIG. 5: The data-to-theory ratio of cross sections as a function of p_T^γ for $\gamma + b + X$ and $\gamma + c + X$ in the regions $y^\gamma y^{\text{jet}} > 0$ and $y^\gamma y^{\text{jet}} < 0$. The uncertainties on the data include both statistical (inner line) and full uncertainties (entire error bar). Also shown are the uncertainties on the theoretical pQCD scales and the CTEQ6.6M PDFs. The scale uncertainties are shown as dotted lines and the PDF uncertainties by the shaded regions. The ratio of the standard CTEQ6.6M prediction to two models of intrinsic charm is also shown.

orders of magnitude in the range $30 < p_T^\gamma < 150$ GeV. The statistical uncertainty on the results ranges from 2% in the first p_T^γ bin to $\approx 9\%$ in the last bin, while the total systematic uncertainty varies between 15% and 28%.

NLO pQCD predictions [20], with the renormaliza-

tion scale μ_R , factorization scale μ_F , and fragmentation scale μ_f , all set to p_T^γ , are compared to data in Fig. 4. The ratios of the measured to the predicted cross sections are shown in Fig. 5.

The uncertainty from the choice of the scale is estimated through a simultaneous variation of all three scales by a factor of two, i.e., to $\mu_{R,F,f} = 0.5p_T^\gamma$ and $2p_T^\gamma$. The predictions utilize CTEQ6.6M PDFs [6], and are corrected for effects of parton-to-hadron fragmentation. This correction for $b(c)$ jets varies from 7.5% (3%) at $30 < p_T^\gamma < 40$ GeV to 1% at $90 < p_T^\gamma < 150$ GeV.

The pQCD prediction agrees with the measured cross sections for $\gamma + b + X$ production over the entire p_T^γ range, and with $\gamma + c + X$ production for $p_T^\gamma < 70$ GeV. For $p_T^\gamma > 70$ GeV, the measured $\gamma + c + X$ cross section is higher than the prediction by about 1.6–2.2 standard deviations (including only the experimental uncertainties) with the difference increasing with growing p_T^γ .

Parameterizations for two models containing intrinsic-charm (IC) have been included in CTEQ6.6 [14], and their ratios to the standard CTEQ predictions are also shown in Fig. 5. Both non-perturbative models predict an increased $\gamma + c + X$ cross section, and for the BHPS model [14] it grows with p_T^γ . The observed difference may also be caused by an underestimated contribution from the $g \rightarrow Q\bar{Q}$ splitting in the annihilation process that dominates for $p_T^\gamma > 90$ GeV [21].

III. DOUBLE PARTON INTERACTIONS IN $\gamma + 3$ JET EVENTS IN $p\bar{p}$ COLLISIONS AT $\sqrt{s} = 1.96$ TEV IN DØ

Many features of high energy inelastic hadron collisions depend directly on the parton structure of hadrons which is still not yet well understood at both the theoretical and experimental levels. Phenomenologically, the proton (or antiproton) may be viewed, in the first naive approximation, as an object composed of three light quarks (or anti-quarks). The study of this structure is founded mainly on the use of a simplified theoretical model which considers high energy inelastic scattering of nucleons as a process involving a single collision of one quark or gluon from one nucleon with one quark or gluon from the other nucleon. In this approach, additional “spectator” partons do not take part in the hard $2 \rightarrow 2$ parton collision and form the so-called “underlying event”.

Another, much less developed, approach is based on models in which there might be more than one hard interaction of parton pairs in one collision of nucleons. Since each incoming hadron is a composite object, consisting of many partons, such a probability should be non-zero. Models with multiple parton collisions have been considered in a few theoretical papers (see refs. inside [22]). It is obvious that the

rate of events with double parton scattering (DPS) depends on how the partons are distributed within the nucleon. The form of the parton spatial distribution and possible correlations between partons is practically unknown. This information is hard to obtain within the present theoretical models based on perturbative QCD and makes a relevant measurement particularly important.

Recently the information about a fraction of the double parton interactions has become very important due to growing Tevatron luminosity and upcoming LHC experiments. It opens the possibility to search for signals from new physics processes for which the DPS events may give a noticeable background.

So far, there have been only four dedicated measurements studying double parton scattering: the AFS experiment in pp collisions at $\sqrt{s} = 63$ GeV [23], UA2 in $p\bar{p}$ collisions at $\sqrt{s} = 630$ GeV [24] and two by CDF in $p\bar{p}$ collisions $\sqrt{s} = 1.8$ TeV [25, 26].

In the present analysis, we use a sample of $\gamma + 3$ jets events collected by the D0 experiment during Run IIa at the integrated luminosity of 1 fb^{-1} in $p\bar{p}$ collisions at $\sqrt{s} = 1.96$ TeV [22]. We determine the fraction of the double parton interactions in a single $p\bar{p}$ collision and also the value of “effective cross section” σ_{eff} . The latter allows, with the known cross sections σ^A and σ^B for two independent parton scatterings A and B, to calculate σ_{DPS} cross section:

$$\sigma_{\text{DPS}} \equiv \frac{\sigma^A \sigma^B}{\sigma_{\text{eff}}} \quad (1)$$

Here the normalization factor σ_{eff} is a parameter that can be directly related to the distance between partons in the nucleon. If the partons are uniformly distributed inside the nucleon (large σ_{eff}), σ_{DPS} will be rather low and, conversely, it should increase for a highly concentrated parton spatial densities (small σ_{eff}). A better energy measurement of photons as compared with jets helps in separating the DP scatterings and allows us to better fix the scale of the main hard interaction.

In the current analysis, to extract σ_{eff} we use a technique that operates only with quantities determined from data analysis and minimizes many theoretical assumptions [22, 26] that were used in some previous measurements. Towards this aim, we measure the number of DP $\gamma + 3$ jets events and the number of $\gamma + 3$ jets events with hard interactions occurring in two separate $p\bar{p}$ collisions. The latter class of events will be called double interactions (DI). Assuming independent (uncorrelated) scatterings in the DP process [27, 28], the DP and DI events should be kinematically identical and differ by just amount of “underlying” energy in one- and two-vertex events. The expression for the effective cross section σ_{eff} can be written in the following form:

$$\sigma_{\text{eff}} = \frac{N_{\text{DI}}}{N_{\text{DP}}} \frac{N_c(1)}{2N_c(2)} \sigma_{\text{hard}}. \quad (2)$$

Here $N_{\text{DI(DP)}}$ is the number of DI(DP) events, $N_c(1)$ and $N_c(2)$ are the numbers of beam crossings with 1 and 2 hard collisions, and σ_{hard} is the cross section of the hard $p\bar{p}$ interaction. We measure σ_{eff} in three bins of the 2nd (ordered in p_T) jet ($p_T^{\text{jet}2}$) which serves as a scale of the additional parton-parton interaction.

We used data collected with the D0 detector during Run IIa which corresponds an integrated luminosity of about $1.02 \pm 0.06 \text{ fb}^{-1}$. The data sets and γ +jets selection criteria, analogous to the previous $p\bar{p} \rightarrow \gamma + \text{jet} + X$ measurements [2, 18], have been used in this analysis.

The main background for the DP events is caused by the $\gamma + 3$ jets events resulting from the single parton (SP) scatterings with hard gluon radiation in the initial or final state $qg \rightarrow q\gamma gg$ or $q\bar{q} \rightarrow g\gamma gg$. The fraction of the DP events is determined in this analysis using a set of variables sensitive to the kinematic configurations of the two independent scatterings of parton pairs. Specifically to the difference between between the p_T imbalances of two pairs in $\gamma + 3$ jets events:

$$S_{p_T} = \frac{1}{\sqrt{2}} \sqrt{\left(\frac{|\vec{p}_T(\gamma, i)|}{\delta p_T(\gamma, i)}\right)^2 + \left(\frac{|\vec{p}_T(j, k)|}{\delta p_T(j, k)}\right)^2} \quad (3)$$

Two other variables, similar to (3), have also been used in the analysis [22] for a cross-check. In the equations above, $\vec{p}_T(\gamma, i)$ and $\vec{p}_T(j, k)$ are the p_T vectors of the total transverse momenta of the two two-body system, and $\delta p_T(\gamma, i)$, $\delta p_T(j, k)$ are the corresponding uncertainties. The pairs are constructed by grouping γ with 3 jets in three possible configurations. The configuration that gives the minimum S is selected for each of the S -family variables. In most events S is minimized by pairing the photon with the leading jet, while the additional jets both come from dijet system or one of them is replaced by the radiation jet.

The ΔS -family variables are allied to the S -family. They are defined as an azimuthal angle between the p_T vectors of the pairs that give a minimum S value:

$$\Delta S = \Delta\phi\left(\vec{p}_T^{\gamma, \text{jet}_i}, \vec{p}_T^{\text{jet}_j, \text{jet}_k}\right) \quad (4)$$

where $\vec{p}_T^{\gamma, \text{jet}_i}$ and $\vec{p}_T^{\text{jet}_j, \text{jet}_k}$ are the total p_T balance vectors of the pairs $(\gamma + \text{jet}_i)$ and $(\text{jet}_j + \text{jet}_k)$ which give minimal S .

The models for signal DP (and DI) events have been constructed directly from data mixing $\gamma + \geq 1$ jet and dijet minimum bias events in the one- (and two-) vertex data [22]. Then the fractions of DP events have been found from analysis of shapes for ΔS distributions in the signal events and data in the adjacent $p_T^{\text{jet}2}$ bins for which we should expect different DP fractions [28]. Fractions of DI events have been found fitting the shapes for ΔS distributions of signal and background events to data. The obtained DP

fractions are shown in Tables I, while the DI fractions vary as 0.189 ± 0.029 at $15 < p_T^{\text{jet}2} < 20 \text{ GeV}$, 0.137 ± 0.027 at $20 < p_T^{\text{jet}2} < 25 \text{ GeV}$ and 0.094 ± 0.025 at $25 < p_T^{\text{jet}2} < 30 \text{ GeV}$.

TABLE I: Fractions of DP events f_{DP} found for the three $p_T^{\text{jet}2}$ intervals (GeV).

$p_T^{\text{jet}2}$	15 – 20	20 – 25	25 – 30
f_{DP}	0.466 ± 0.041	0.334 ± 0.023	0.235 ± 0.027

TABLE II: Effective cross section σ_{eff} (mb) found in the three $p_T^{\text{jet}2}$ intervals (GeV).

σ_{eff}	15 – 20	20 – 25	25 – 30
$p_T^{\text{jet}2}$	16.2 ± 2.8	13.8 ± 3.1	11.5 ± 4.7

The resulting values of σ_{eff} with total (systematic \oplus statistics) uncertainties are given in Table II for the three $p_T^{\text{jet}2}$ bins. The total systematic uncertainty varies between 19% and 31% and is mainly caused by the determination of the DI and DP fractions as well as by the ratios of the DP/DI selection efficiencies.

One can see that the obtained σ_{eff} values in different jet p_T bins agree with each other within their uncertainties. Using this fact and also that the uncertainties in different jet p_T bins have very small correlation, we can calculate the σ_{eff} value averaged over the three jet p_T bins. It gives us

$$\sigma_{\text{eff}}^{\text{aver.}} = 15.1 \pm 1.9 \text{ mb.} \quad (5)$$

It is worth mentioning that the obtained average value is in the range of those found in previous analogous measurements [24]–[26]. This closeness may indicate a tendency for a stable behavior of σ_{eff} with respect to the transverse momentum of the jet produced in the second parton-parton interaction.

IV. CONCLUSION

The presented measurements of production cross sections for γ +jet, γ +heavy flavour jet and study of the events with double parton scatterings provide precision tests of perturbative QCD as well as information on the fundamental structure of the nucleon; momentum and spatial distributions of partons in the nucleon. In addition to these important aspects of QCD dynamics, this knowledge should be very helpful for many searches for new physics since, for example, γ +jet and $\gamma + b(c)$ jets are noticeable components for the background to many Higgs boson decay modes (e.g. $h \rightarrow \gamma\gamma, bb$) as well to extra dimensions with graviton ($G \rightarrow ee, \gamma\gamma$) and technicolor (e.g. $\omega_T \rightarrow \gamma\pi_0, a_T^\pm \rightarrow \gamma\pi^\pm$ with $\pi^0 \rightarrow b\bar{b}, \pi^\pm \rightarrow b\bar{c}, \bar{b}c$)

[29]. Knowledge of parton matter structure and parton correlations being extremely valuable *per se* is also important for understanding multijet production

characteristic for many physics final states, especially expected in many SUSY models [21].

-
- [1] J.F. Owens, Rev.Mod.Phys. **59** (1987)465.
 [2] DØ Collaboration, V. Abazov *et al.*, Phys. Lett. B **666**, (2008)435.
 [3] DØ Collaboration, V. Abazov *et al.*, Nucl. Instrum. Methods, Phys. Res., **A565** (2006)463.
 [4] G.C. Blazey *et al.*, arXiv:hep-ex/0005012 (2000).
 [5] R. Barlow, C. Beeston, Comp.Phys.Comm. **77** (1993)219-228.
 [6] W.K. Tung *et al.*, JHEP 0702, 53 (2007).
 [7] S. Catani, M. Fontannaz, J.Ph. Guillet and E. Pilon, JHEP 0205 (2002), 028, hep-ph/0204023.
 [8] L. Bourhis, M. Fontannaz, J.P. Guillet, Eur.Phys.J. **C2** (1998)529, hep-ph/9704447.
 [9] This scale choice is suggested by M. Fontannaz and J. P. Guillet. Private communication.
 [10] UA2 Collaboration, J. Alitti, *et al.*, Phys.Lett. **263B** (1991)544.
 [11] CDF Collaboration, D. Acosta, *et al.*, Phys.Rev. **D65**(2002)112003.
 [12] DØ Collaboration, V. Abazov *et al.*, Phys.Lett. **B639** (2006)151-158.
 [13] B. Bailey, E.L. Berger, L.E. Gordon, Phys.Rev. **D54** (1996)1896-1907, hep-ph/9602373; E.L. Berger, L.E. Gordon, Phys.Rev. **D54** (1996) 2279-2294, hep-ph/9512343.
 [14] J. Pumplin *et al.*, Phys.Rev. **D75** (2007)054029, hep-ph/0701220.
 [15] S.J. Brodsky, B. Kopeliovich, I. Schmidt, J. Soffer, Phys. Rev. D **73**, 113005 (2006).
 [16] H.J. He, C.P. Yuan, Phys. Rev. Lett. **83**, 28 (1999); C. Balazs, H.J. He, C.P. Yuan, Phys. Rev. D **60**, 114001 (1999).
 [17] K.A. Assamagan, *et al*, hep-ph/0406152.
 [18] DØ Collaboration, V. Abazov *et al.*, Phys. Rev. Lett. **102**, 192002 (2009).
 [19] T. Scanlon, Ph.D. thesis, FERMILAB-THESIS-2006-43.
 [20] T.P. Stavreva, J.F. Owens, arXiv:0901.3791 [hep-ph].
 [21] C. Amsler *et al.*, Phys.Lett. **667B** (2008)1.
 [22] DØ Collaboration, V. Abazov *et al.*, D0 Conference Note 5910-CONF.
 [23] AFS Collaboration, T. Akesson *et al.*, Z.Phys. C **34** (1987) 163.
 [24] UA2 Collaboration, J. Alitti *et al.*, Phys. Lett. B **268** (1991) 145.
 [25] CDF Collaboration, F. Abe *et al.*, Phys. Rev. D **47** (1993) 4857.
 [26] CDF Collaboration, F. Abe *et al.*, Phys. Rev. D **56** (1997) 3811.
 [27] T. Sjostrand and P.Z. Scands, JHEP (2004) **0403**.
 [28] B. Humpert, Phys. Lett. B **131** (1983) 461; B. Humpert and R. Odorico, Phys. Lett. B **154** (1985) 211.
 [29] E. Eighten, K. Lane, J. Womersley, FERMILAB-PUB-97/116-T, Phys.Lett. **B405** (1997)305.